

Birefringence in optical waveguides made by silicon nanocrystal superlattices

F. Riboli,^{a)} D. Navarro-Urrios, A. Chiasera, N. Daldosso, and L. Pavesi

Dipartimento di Fisica, Università di Trento, via Sommarive 14, I-38050 Povo (Trento), Italy

C. J. Oton

Departamento de Física Básica, University of La Laguna, Avda. Astrofísico Fco. Sánchez, La Laguna, 38204 Spain

J. Heitmann, L. X. Yi, R. Scholz, and M. Zacharias

Institute of Microstructure Physics, Weinberg 2, 06120 Halle, Germany

(Received 11 March 2004; accepted 10 June 2004)

We investigate the optical properties of planar waveguides where the core layer is formed by a silicon nanocrystals (Si-nc)/SiO₂ superlattice. M-line measurements of the different waveguides yield the mode indices, which can be modeled by assuming anisotropic optical properties of the core layer. This anisotropy is related to the superlattice, i.e., it is a form birefringence. By modeling the m-line measurements with the structural data obtained by transmission electron microscopy analysis, we determine for each waveguide the value of the form birefringence, an upper limit of the nanocrystals size and their refractive index. Values of the form birefringence as high as 1% have been found. © 2004 American Institute of Physics. [DOI: 10.1063/1.1779969]

Low-dimensional silicon, as silicon nanocrystals (Si-nc), is a material with extremely interesting optoelectronic properties.¹ Efficient room-temperature emission which can be also electrically excited,² nonlinear optical properties with increased third-order nonlinear susceptibility,³ and stimulated emission⁴ are just some examples. The usual process to form Si-nc is by a thermally induced phase separation of Si and SiO₂. An undesired result of this process is the large size dispersion of the Si-nc. Recently, an approach to reduce the size dispersion has been proposed.⁵ This is based on the deposition of nanometer-thick multilayers of SiO₂ and SiO_y ($y \approx 2$). After thermal annealing at a high temperature, a phase separation occurs only in the SiO_y layers where Si-nc form with a typical size constrained to the SiO_y thickness. In this way, a very narrow dispersion of Si-nc sizes is achieved.⁵ The final result is a stack of layers of SiO₂ and Si-nc rich SiO₂, called a superlattice (SL) in the following.

Si-nc rich samples have homogeneous optical properties because the Si-nc sizes are much smaller than the wavelength of light. Their refractive index depends on the Si-nc sizes and concentration. Si-nc-based waveguides where the cladding layers are formed by SiO₂ and the core layer is rich in Si-nc can be formed. Usually Si-nc are randomly arranged in the waveguide core and the resulting optical constants are isotropic. On the contrary, in the Si-nc/SiO₂ SL, there is a stack of alternate low and high refractive index nanometer-thick layers, which forms an homogeneous medium with a high *form birefringence*. In this system, the optical constants are uniaxial with ordinary n_o and extraordinary n_e refractive indices. A negative material birefringence $\beta = (n_e - n_o)/n_o$ is predicted theoretically.^{6,7} In this letter, we confirm this theoretical prediction and report on the optical characterization and modeling of the form birefringence of Si-nc/SiO₂ SLs. Waveguides were produced in a conventional evaporation system by deposition of the layered structure on a quartz

substrate. Rotation of the substrate enables high deposition homogeneity over the whole wafer. More details on the growth method and apparatus are reported in Ref. 5. Briefly, the SL structure is formed by repetitive depositions of nanometer thick SiO_y ($y \approx 1$) and SiO₂ layers. The SiO_y layers were deposited by reactive evaporation of SiO powders in a vacuum, while for SiO₂ an additional oxygen pressure of 1×10^{-4} mbar was used. The substrate temperature was 100 °C. The stoichiometry was measured by Rutherford backscattering method using equally deposited thick SiO and SiO₂ films. After deposition, annealing at 1100 °C in a N₂ atmosphere for 1 h induces the formation of Si-nc. Four planar waveguides (named A, B, C, D) have been investigated, see Table I. They differ mainly for the thickness of the SiO_y layers in the SL. TEM (transmission electron microscopy) studies show that during the annealing, oxidation takes place at the interfaces between the SL and the quartz substrate or the air because the quartz substrate was not preannealed to drive out residual water. Such oxidation consumes a few Si-nc/SiO₂ periods replacing them with an amorphous SiO_x

TABLE I. Nominal growth parameters and parameters extracted from cross-sectional TEM images for the studied waveguides. d_{SiO_y} is the nominal thickness of the silicon oxide deposited layers, d_{SiO_2} is the nominal thickness of the silica layers, and N_{Si} and N_{SiO_2} are the number of SiO and SiO₂ layers in the active SL.

Waveguide name	A	B	C	D
(a) Nominal parameters				
d_{SiO_y} (nm)	2	3	4	5
d_{SiO_2} (nm)	5	5	5	5
$N_{\text{Si}}/N_{\text{SiO}_2}$	45/46	45/46	45/46	45/46
(b) TEM data				
Bottom SiO _x thickness (nm)	25	25	71	11
Superlattice thickness (nm)	152	186	214.5	295.2
Top SiO _x thickness (nm)	69.5	68	14	25
Total measured thickness (nm)	247	270	291	331

^{a)}Electronic mail: riboli@science.unit.it

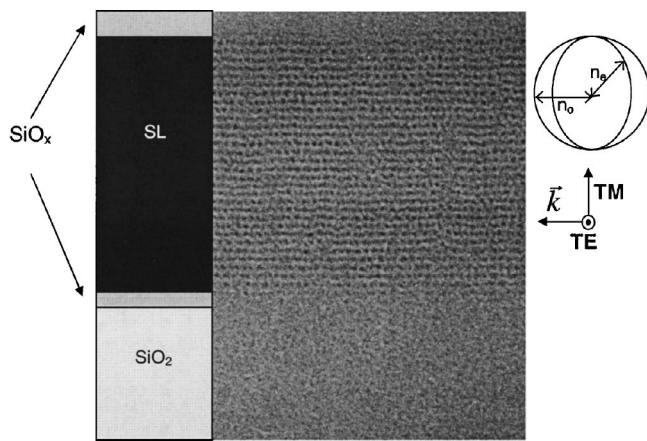


FIG. 1. TEM image of waveguide B (right) and schematization of the structure used in the simulations (left). \mathbf{k} is the propagation vector of the guided wave. TE and TM define the two polarizations of the light. It is also showed the indexes ellipse.

layer ($x \approx 2$) whose thickness is sample dependent. Hence, the final structure of the waveguides is a sequence of four layers: A quartz cladding, a bottom SiO_x layer, a Si-nc/ SiO_2 SL core layer, and a top SiO_x layer (see Fig. 1). Their thickness is determined by TEM and reported in Table I. By dividing the measured thickness of the SL core by the counted number of SL periods, the SL period thickness can be estimated.

To characterize the optical properties of the waveguides, standard m-line measurements have been performed with two wavelengths: $\lambda = 633$ and 543 nm. Representative m-line measurements on waveguide D are shown in Fig. 2 and a summary of the results on all the waveguides is reported in Table II. Each data point is an average of repeated measurements on various points on the waveguide. The waveguides were single-mode waveguides.

As expected, the effective modal indices n_{TE} and n_{TM} and the modal birefringence ($B = n_{\text{TE}} - n_{\text{TM}}$) depend on both the wavelength (due to index dispersion) and the Si-nc size (due to a variation in the overall Si content of the SL layer). Usually, n_{TE} and n_{TM} can be simulated by using a waveguide simulation code, where the Si-nc rich layer is described by a single refractive index. In our data, because of the multilayer structure which causes anisotropy in the optical constants,

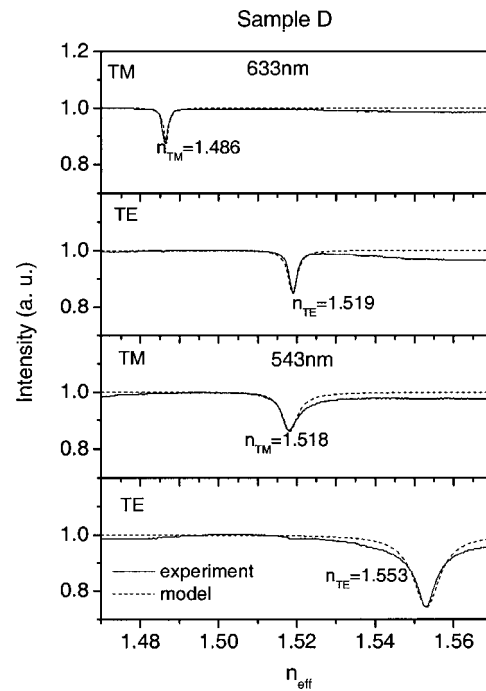


FIG. 2. M-line measurements for the TE and TM polarization on waveguide D (solid) together with a simulation (dash) made using the extracted ordinary and extraordinary indices.

i.e., birefringence, we have to use two indices in the simulation: An ordinary (n_o) and an extraordinary (n_e) refractive one. An estimation of these indices can be done by using:^{8,9}

$$n_0^2 = \frac{N_{\text{NS}} n_{\text{NS}}^2 d_{\text{NS}} + N_{\text{SiO}_2} n_{\text{SiO}_2}^2 d_{\text{SiO}_2}}{d_{\text{NS}} + d_{\text{SiO}_2}}, \tag{1a}$$

$$\frac{1}{n_e^2} = \frac{d_{\text{NS}} + d_{\text{SiO}_2}}{\frac{N_{\text{NS}} d_{\text{NS}}}{n_{\text{NS}}^2} + \frac{N_{\text{SiO}_2} d_{\text{SiO}_2}}{n_{\text{SiO}_2}^2}}, \tag{1b}$$

where the average is performed on the SL layer assuming a periodic structure of N_{NS} layers with refractive index n_{NS} and thickness d_{NS} (the Si-nc rich layers), and N_{SiO_2} with a refractive index n_{SiO_2} and thickness d_{SiO_2} (the SiO_2 layers). This

TABLE II. Summary of the different waveguide parameters extracted from the m-line measurements, simulations and TEM images. $n_{\text{TE}}(n_{\text{TM}})$ is the modal index for TE (TM) mode, B is the modal birefringence, $\Gamma_{\text{TE}}(\Gamma_{\text{TM}})$ is the optical filling factor in the waveguide core for TE (TM) mode, and n_o and n_e are the ordinary and extraordinary effective indices of the core layer. $\beta = 100 * (n_e - n_o) / n_o$ is the material birefringence.

	Waveguide B		Waveguide C		Waveguide D	
	633 nm	543 nm	633 nm	543 nm	633 nm	543 nm
n_{TE}	1.462±0.001	1.473±0.001	1.476±0.001	1.497±0.001	1.519±0.001	1.553±0.001
n_{TM}	1.456±0.002	1.463±0.001	1.458±0.001	1.471±0.001	1.486±0.001	1.518±0.001
$B = n_{\text{TE}} - n_{\text{TM}}$	0.006±0.003	0.010±0.002	0.018±0.002	0.026±0.002	0.033±0.002	0.035±0.002
$\Gamma_{\text{TE}}(\%)$	27	42	44	59	72	81
$\Gamma_{\text{TM}}(\%)$	3	23	10	35	56	73
n_{SiO_x}	1.4755	1.4790	1.4755	1.4790	1.4755	1.4790
n_o	1.564±0.003	1.568±0.002	1.600±0.002	1.611±0.002	1.621±0.001	1.643±0.001
n_e	...	1.567±0.005	1.581±0.004	1.596±0.002	1.603±0.001	1.624±0.001
$\beta(\%)$...	-0.5±0.5	-1.1±0.3	-1.0±0.3	-1.1±0.1	-1.1±0.1
d_{NS}	...	2.2±0.3 nm	3.1±0.2 nm	3.3±0.1 nm	4.4±0.1 nm	4.4±0.1 nm

model fixes the condition $n_e < n_o$, i.e., negative birefringence.

As sample D has a negligible thickness of the SiO_x layers (see Table I), we modeled it as a three-layer waveguide: Air, quartz, and the SL core layer. It was assumed that $n_{\text{SiO}_2} = 1.458$ or 1.457 at 543 or 633 nm. Simulation of the m-line data yields n_o and n_e . From n_o , n_e , and Eq. (1), d_{NS} , d_{SiO_2} , and n_{NS} are found with the only constraint that $d_{\text{SiO}_2} + d_{\text{NS}}$ should be equal to the SL period measured by TEM. The procedure is different for the other waveguides because of the thickness of the SiO_x layers (Table I). The refractive index n_{SiO_x} of such layers is not known. As in the TEM images, no contrast between the SiO_x layers and the quartz substrate is observed, we make the conservative assumption of taking $x \leq 2$, i.e., $n_{\text{SiO}_x} \approx n_{\text{SiO}_2}$.¹⁰ Moreover, if we consider that the composition of the deposited SiO_y layers in the SL and the annealing temperature are the same for all the waveguides, we can assume the very same n_{NS} for all waveguides, that found for waveguide D. In this way, a pair of n_o and n_e which models the m-line measurements and solves Eq. (1) can be obtained by using as free parameters d_{NS} and d_{SiO_2} , only. In Table II, the results of this procedure are reported. The material birefringence values we found are robust with respect to variation in n_{SiO_x} .

Waveguide D supports both the transverse electric (TE) and transverse magnetic (TM) modes with the highest filling factors. The modeling of the complete waveguide structure, with the two thin SiO_x layers, yields a value for the birefringence parameter $\beta \approx -1.1\%$. The estimated refractive index n_{NS} is 1.705 at 633 nm and 1.735 at 543 nm. Waveguide C has smaller filling factors but similar $\beta \approx -1.1\%$ as waveguide D. Waveguide B at 633 nm shows a weak optical confinement of the TE mode and an extremely weak for the TM mode because of the small thickness of the SL core. No reliable birefringence value can be extracted for this wavelength. At 543 nm, both TE and TM modes are well confined in waveguide B. The modeling yields a $\beta \approx -0.5\%$, lower than that for the other waveguides. Waveguide A does not support any modes due to the significant large oxidation of the SL layers.

In order to make another check of the model, we measured other Si-nc-rich waveguides obtained by ion implantation and annealing.¹¹ M-line measurements yield modal birefringence in the 0.02 – 0.01 range, i.e., in the same range as those found in this letter. However, by fitting the m-line measurements, we found $n_o = n_e$, i.e., the core layer of the waveguides behaves as an isotropic media with refractive index in the range, from 1.55 to 1.65 . This strongly supports the *form* nature of the observed birefringence in the SL-based waveguides.

It is worth noting that modeling of the waveguide data yields the same d_{NS} for the two wavelengths used: $d_{\text{NS}} = 4.4$, 3.3 , and 2.2 nm for the D, C, and B waveguide, respectively. These numbers are consistent with the photoluminescence measurements reported elsewhere¹² and the nominal growth parameters (Table I).

The extracted n_{NS} value needs some comments. By making use of the Bruggemann approximation for isotropic me-

dia, we can estimate refractive index value of the Si-nc-rich layer.⁸ Let us assume that all the excess Si in the deposited SiO_y layer is consumed in the formation of the Si-nc. If a perfect phase separation in Si-nc and SiO_2 is assumed, this corresponds to a Si volumetric fraction of 30% . By using the Bruggemann approximation, we found $n = 1.97$ at 633 nm and 2.01 at 543 nm, where we have taken the refractive index of bulk silicon for the Si-nc. It is possible to refine this estimation by taking into account that the refractive index of the Si-nc can be lower than that of Si bulk.^{13,14} In any case, the obtained values are higher than n_{NS} leading us to think that either the composition of the matrix is not pure SiO_2 (e.g., contamination with N or other species is present) or not all excess Si is spent in the formation of nanocrystals. Evidence of an intermediate region of amorphous SiO_x coating the Si-nc surface has been reported in literature.¹⁵ Energy-filtered TEM measurements show that the quantity of Si in the Si-nc is lower than the quantity of excess Si in the deposited SiO_x .¹⁶ Both observations support our results.

In conclusion, we have found a negative form birefringence of about 1% in a set of planar waveguides whose active core was a periodic repetition of a Si-nc-rich SiO_2 layer and a SiO_2 layer. This form birefringence could be exploited in optical devices, such as wavelength filters, coherence modulators, and polarization converters.¹⁷ Its modeling allows the determination of different structural and optical parameters of the SLs. As in other reports, we found a lower Si-nc concentration than expected from pure stoichiometric arguments.

¹S. Ossicini, F. Priolo, and L. Pavesi, *Light-Emitting Silicon for Microphotonics* (Springer, New York, 2004).

²A. Irrera, D. Pacifici, M. Miritello, G. Franzò, F. Priolo, F. Iacona, D. Sanfilippo, G. Di Stefano, and P. G. Fallica, *Appl. Phys. Lett.* **81**, 1866 (2002).

³G. Vijaya Prakash, M. Cazzanelli, Z. Gaburro, L. Pavesi, F. Iacona, G. Franzò, and F. Priolo, *J. Mod. Opt.* **49**, 719 (2002).

⁴L. Dal Negro, M. Cazzanelli, L. Pavesi, S. Ossicini, D. Pacifici, G. Franzò, F. Priolo, and F. Iacona, *Appl. Phys. Lett.* **82**, 4636 (2003).

⁵M. Zacharias, J. Heitmann, R. Scholz, U. Kahler, M. Schmidt, and J. Bläsing, *Appl. Phys. Lett.* **80**, 661 (2002).

⁶D. Bergman, *Phys. Rep.* **43**, 377 (1978).

⁷J. Kang, G. I. Stageman, C. H. Huang, D. L. Li, H. H. Lin, H. C. Chang, and C. C. Yang, *IEEE Photonics Technol. Lett.* **7**, 769 (1995).

⁸D. E. Aspnes, *Am. J. Phys.* **50**, 704 (1982).

⁹S. Ohke, T. Umeda, and Y. Cho, *Opt. Commun.* **56**, 235 (1985).

¹⁰S. M.A. Durrani, M. F. Al-Kuhaili, and E. E. Khawaja, *J. Phys.: Condens. Matter* **15**, 8123 (2003).

¹¹B. Garrido, M. López, C. Garcia, A. Pérez-Rodríguez, J. R. Morante, C. Bonafos, M. Carrada, and A. Claverie, *J. Appl. Phys.* **91**, 798 (2002).

¹²M. Cazzanelli, D. Navarro-Urrios, F. Riboli, N. Daldosso, L. Pavesi, J. Heitmann, L. X. Yi, R. Scholz, M. Zacharias, and U. Gösele, *J. Appl. Phys.* (to be published).

¹³J. A. Moreno, B. Garrido, P. Pellegrino, C. Garcia, R. Ferré, J. R. Morante, C. Bonafos, P. Marie, F. Gourbilleau, and R. Rizk.

¹⁴M. Lannoo, C. Delerue, and G. Allan, *Phys. Rev. Lett.* **74**, 3415 (1995).

¹⁵N. Daldosso, M. Luppi, S. Ossicini, E. Degoli, R. Magri, G. Dalba, P. Fornasini, R. Grisenti, F. Rocca, L. Pavesi, S. Boninelli, F. Priolo, C. Bongiorno, and F. Iacona, *Phys. Rev. B* **68**, 085327 (2003).

¹⁶F. Iacona, C. Bongiorno, C. Spinella, S. Boninelli, and F. Priolo, *J. Appl. Phys.* **95**, 3723 (2004).

¹⁷*Silicon Photonics*, edited by Lorenzo Pavesi and David G. Lockwood (Springer, Berlin, 2004).